Malaysian Journal of Analytical Sciences (MJAS)



Published by Malaysian Analytical Sciences Society

INHIBITION EFFECTS OF TRIDENTATE HYDRAZONE LIGANDS AS CORROSION INHIBITORS ON MILD STEEL IN SATURATED CO₂ ENVIRONMENT

(Kesan Perencatan Ligan Hidrazon Tridentat Sebagai Perencat Kakisan Pada Keluli Lembut Dalam Persekitaran CO₂ Tepu)

Balqis Auni Badrul Hisyam¹, Zainiharyati Mohd Zain², Nurulfazlina Edayah Rasol^{1,3} and Amalina Mohd Tajuddin ^{1,3*}

¹Faculty of Applied Sciences, Universiti Teknologi MARA (UiTM), 40450 Shah Alam, Selangor, Malaysia ²Electrochemical Material and Sensor (EMaS), Universiti Teknologi MARA (UiTM), 40450 Shah Alam, Selangor, Malaysia ³Atta-ur-Rahman Institute for Natural Product Discovery (AuRIns), UiTM Puncak Alam, 42300, Bandar Puncak Alam, Selangor, Malaysia

*Corresponding author: amalina9487@uitm.edu.my

Received: 15 September 2023; Accepted: 25 November 2023; Published: 28 February 2024

Abstract

Two tridentate hydrazone ligands (AL01, AL02) were synthesized by condensation of an aldehyde and two hydrazides, benzohydrazide and 2-hydroxybenzohydrazide with OH substituent at the ortho position of the benzene ring. They were characterized using melting point, FTIR, NMR, elemental analysis, UV-Vis as well as mass spectroscopy. The formation of hydrazone ligands was confirmed by the appearance of v(C=N) peak in the range of 1608 to 1648 cm⁻¹. The significant peak of N-H protons for AL01 and AL02 appeared at 8.82 and 8.41 ppm respectively, while the peak of phenolic proton (O-H) for AL01 was found at 12.28 ppm. Two peaks were observed in the wavelength range of 198-220 nm that can be attributed to π - π^* (C=C) and $n-\pi^*_{(C=C)}$ transitions of aromatic benzene, while the peaks for $\pi-\pi^*_{(C=N)}$ were observed in the range of 297–303 nm. The mass-tocharge (m/z) [M+H]⁺ values of AL01 and AL02, which are 242.09 and 226.10, respectively, further confirmed their structures. The effectiveness of hydrazone ligands as corrosion inhibitors on mild steel in 3.5% NaCl solution saturated with CO2 was examined using polarization and electrochemical impedance spectroscopy (EIS). The elemental constituents of the protective layer forms on mild steel immersed in the solution were further observed using scanning electron microscopy (SEM) coupled with energy-dispersive X-Ray (EDX)). Therefore, new corrosion inhibitors of tridentate hydrazone ligands, AL01 and AL02 were successfully synthesized and characterized using FTIR, NMR, elemental analysis, mass spectroscopy and UV-Vis. From polarization and EIS study, AL01 can be concluded to have higher inhibition efficiency, 84.30% at 500 ppm concentration compared to AL02, 74.90%. SEM-EDX analysis has confirmed the formation of the inhibitors' layer on mild steel as the surface of the mild steel immersed in solution with the presence of inhibitors have a smoother surface compared to that of untreated mild steel in 3.5% NaCl solution saturated with CO₂.

Keywords: CO₂, corrosion inhibitor, mild steel, protective layer, tridentate hydrazone

Hisyam et al.: INHIBITION EFFECTS OF TRIDENTATE HYDRAZONE LIGANDS AS CORROSION INHIBITORS ON MILD STEEL IN SATURATED CO₂ ENVIRONMENT

Abstrak

Dua ligan hidrazon tridentat (AL01, AL02) telah disintesis melalui pemeluwapan antara aldehid dan dua hidrazida, benzohidrazida dan 2-hidroksibenzohidrazida, dengan kumpulan pengganti OH pada kedudukan orto hidrazida. Mereka dicirikan menggunakan takat lebur, FTIR, NMR, analisis unsur, UV-Vis serta spektroskopi jisim. Pembentukan ligan hidrazon telah disahkan oleh kemunculan puncak v(C=N) dalam julat 1608 hingga 1648 cm⁻¹. Puncak utama proton N-H untuk AL01 dan AL02 masing-masing muncul pada 8.82 dan 8.41 ppm, manakala puncak proton fenolik (O-H) untuk AL01 didapati pada 12.28 ppm. Dua puncak diperhatikan dalam julat 198-220 nm yang boleh dikaitkan kepada peralihan π-π*_(C=C) dan n-π*_(C=C) Kumpulan benzena aromatik manakala pucak bagi peralihan π - π *(C=N) telah diperhatikan dalam julat 297-303 nm. Nilai jisim-ke-cas (m/z) [M+H]+ bagi AL01 dan AL02, iaitu 242.09 dan 226.10, masing-masing, memberikan pengesahan lanjut tentang strukturnya. Keberkesanan ligan hidrazon sebagai perencat kakisan pada keluli lembut dalam larutan NaCl 3.5% tepu dengan CO2 telah diperiksa menggunakan polarisasi dan spektroskopi impedans elektrokimia (EIS). Kehadiran unsur pada lapisan pelindung yang terbentuk pada keluli lembut yang direndam dalam larutan diperhatikan selanjutnya menggunakan mikroskop elektron pengimbasan (SEM) ditambah dengan X-Ray penyebaran tenaga (EDX). Oleh itu, perencat kakisan baru, ligan hidrazon tridentat, AL01 dan AL02 telah berjaya disintesis dan dicirikan menggunakan FTIR, NMR, analisis unsur, spektroskopi jisim dan UV-Vis. Daripada kajian polarisasi dan EIS, dapat disimpulkan bahawa AL01 mempunyai kecekapan perencatan yang lebih tinggi iaitu, 84.30% pada 500 ppm berbanding AL02 iaitu, 74.90%. Analisis SEM-EDX telah mengesahkan pembentukan lapisan perencat pada keluli lembut kerana permukaan keluli lembut dengan kehadiran perencat mempunyai permukaan yang lebih licin berbanding keluli lembut yang tidak dirawat dengan perencat kakisan dalam larutan 3.5% NaCl tepu dengan CO2.

Kata kunci: CO₂, perencat kakisan, keluli lembut, lapisan pelindung, hidrazon tridentat

Introduction

Corrosion is a common natural interaction between a pure metal and its surroundings where the metal tends to revert to its stable condition i.e., a compounded state, and the substance deteriorates because of energy being released in the process [1, 2]. It has a significant influence on a variety of machinery, infrastructures, industrial plants, and human life. Many things can suffer serious damage from corrosion, and the costs of the destruction are substantial [3]. A previous study by Tamalmani et al., stated that corrosion has been highlighted as one of the key causes of oil and gas infrastructure problems. Internal pipeline is one of the widely used means for transporting resources in the oil and gas sector, however, internal pipeline corrosion has seemed to represent a substantial threat [4]. It has been acknowledged that pipeline corrosion is primarily brought on by the presence of carbon dioxide (CO₂) as the major corrosive medium which commonly happens during transportation of hydrocarbons in the pipeline. Due to the solubility of CO₂ in water and brine (NaCl solution), the steel and the contacting aqueous phase undergo electrochemical process resulted in carbonic acid (H₂CO₃) formation, that leads to severe corrosion in pipelines [4-6].

Mild steel is often utilized as a raw material for the construction of pipelines, nevertheless, due to its premature failure and degradation, a gross expenditure of billions of dollars has been incurred worldwide. These costs include replacement, maintenance, and lost productivity since mild steel is an essential component in an infrastructure, which includes pipelines, port facilities, and bridges [7]. This low-carbon steel is widely sought-after for high temperature applications, such as petrochemical processes and pipeline construction, due to its malleability and lack of brittleness. Mild steel is widely used in the oil and gas industries for transporting gases and liquids over long distances in pipelines from their sources to the consumers [8], despite having a low corrosion resistance because of its availability, affordability, and hardness [1]. Moreover, mild steel consists of porous regions within its structure that make it more prone to corrosion, especially in corrosion-aggressive environments such chemical industries, the ocean, and polluted environments [9, 10]. Transportation of crude oil in pipelines for instance, often comes naturally with impurities such CO₂, water, and oxygen, which are thought to be the main causes of corrosion in pipelines. Studies found that since CO₂ dissolves in aqueous solution to generate weak carbonic acid (H₂CO₃) [8, 11, 12], which is considered to be the most hazardous

type of acids to carbon steel, a combination of CO_2 with water indicates a serious corrosion problem. However, the condition gets worsen with the combination of CO_2 with brine solution (NaCl). A study reported by Almeida et al., found that the corrosion rate of steel in distilled water was 28.3 mm/y while in brine solution after being immersed for 30 minutes was 119 mm/y [13].

Therefore, investigations were conducted, and it was discovered that using corrosion inhibitors could be one of the strategies to resolve this problem since it is easy to put into application, affordable, and under control [10]. However, it was also discovered that the inorganic inhibitors used in passivation processes, such as nitrates, chromates, and derivatives of azole and thiourea, were hazardous to both humans and the environment. Additional research on effective, environment-friendly inhibitors that can provide a protective layer on metals is required to address these problems to mitigate the rate of corrosion [14]. Corrosion inhibitors need at least one polar group, such as heteroatoms that can facilitate the process of adsorption in an acidic environment to be able to bond to the metal surface. Additionally, the effect of corrosion inhibition may be enhanced by changing the molecule's size. orientation, and geometry. Aforementioned, organic compounds with unsaturated bonds or heteroatoms like O, N, and S as well as functional groups like -NH, NN, CN-, and CHO frequently work well as corrosion inhibitors [15].

Due to their unique chemical properties, hydrazones, which belong to a special family of organic molecules, have several biological and therapeutic uses. For example, hydrazone-based inhibitors derived from non-steroidal anti-inflammatory medicines (NSAIDs) such mefenamic acid, naproxen, and ibuprofen have been produced, which have shown to be effective against steel corrosion [16]. The most advantageous property of hydrazones is their high reactivity because of the azomethine group, which has two nitrogen atoms with nucleophilic properties and a carbon atom with both electrophilic and nucleophilic properties [17]. In addition, hydrazone-based inhibitors have also been

identified as "green corrosion inhibitors" that prevent corrosion by adsorption on the metal surface since they are non-toxic, inexpensive, and biodegradable [18].

Hence, in this study, new corrosion inhibitors of tridentate hydrazone ligands without and with the presence of OH substituent at the *ortho* position of the benzene ring were synthesized, characterized, and evaluated as organic corrosion inhibitors. To the best of our knowledge, no reports on using AL01 and AL02 as corrosion inhibitors are available. Therefore, the relationship between the absence and presence of electron-donating group (-OH) [19] with the inhibition efficiency and corrosion rate of the mild steel is reported.

Materials and Methods

Materials

2-Pyridinecarboxaldehyde, 2-hydroxybenzohydrazide, benzohydrazide, and methanol purchased from commercial suppliers were used without further purification. Melting point determination in triplicate was carried out in glass capillary tubes using Buchii-B454 and the percentage compositions of the elements C, H and N of the compounds were determined by using Thermo Scientific Flash 2000 Elemental Analyzer with sulphanilamide as the standard. Fourier-transform infrared spectra (FTIR) were recorded using Perkin-Elmer FT-IR 1600 spectrometer by preparing samples as KBr discs. ¹H NMR spectra were recorded on Bruker Avance 600 MHz NMR spectrometer in deuterated solvents, DMSO and CDCl₃. UV-Vis spectra were obtained in acetonitrile (5x10⁻⁵ M) in the 190-450 nm range Perkin Elmer Lambda 25 UV/Vis Spectrometer. Mass spectral data are measured in 1:1 ratio of acetonitrile: H₂O at concentration of 10 ppm using Thermo Scientific Vanquish Horizon UHPLC system fitted with Thermo Scientific TM Orbitrap Fusion Tribrid. The column used was Accucore TM Vanquish C18 (2.1 x 100 mm, 1.5 µm) at 37 °C.

Synthesis of tridentate hydrazone ligands

Scheme 1 shows the synthesis reaction for tridentate hydrazone ligands.

Scheme 1. Overall reaction between hydrazides and aldehyde

Synthesis of (E)-2-hydroxy-N'-(pyridin-2-ylmethylene)benzohydrazide (AL01)

2-Pyridinecarboxaldehyde (5 mmol, 0.5356 g) and 2hydroxybenzohydrazide (5 mmol, 0.7608g) were dissolved in methanol (20 mL), and the mixture was heated under reflux for 30 minutes. The colorless solid obtained was filtered using vacuum pump and washed with ice cold methanol and air dried at room temperature. Yield: 83.5%. IR (KBr pellet, cm⁻¹): v(N-H) 3242 cm^{-1} , $v(C=N) 1608 \text{ cm}^{-1}$, v(C=N) (pyridine) 1542 cm^{-1} , v(C=O) and 1630 cm^{-1} ¹H NMR (500 MHz, CDCl₃) δ 12.28 (s, 1H), 8.82 (s, 1H), 7.97 (td, J = 7.8, 1.8 Hz, 1H), 7.69 (dd, J = 7.6 Hz, 1H), 7.64 - 7.54 (td, 1H), 7.58 - 7.54 (dd, 1H), 7.51 (dd, J = 1.6 Hz, 1H), 7.49-7.43 (td, 1H), 7.09 - 7.04 (td, 1H), 7.01 - 6.94 (dd, 1H), 2.19 (s, 1H). Anal. Calc. (%) For C₁₃H₁₁N₃O₂: C, 64.72 H, 4.60; N, 17.42. Found (%): C, 65.21; H, 4.66; N, 17.75.

Synthesis of (E)-N'-(pyridin-2-ylmethylene) benzohydrazide (AL02)

A mixture of 2-pyridinecarboxaldehyde (5 mmol, 0.5356 g) and bezohydrazide (5 mmol, 0.6808g) was prepared in 20 mL methanol. The reaction mixture was refluxed for 4 hours, and the solvent was concentrated using rotary evaporator. The concentrated product was cooled at room temperature until colorless precipitate formed. Yield: 66.7%. IR (KBr pellet, cm⁻¹): ν (N-H) 3402 cm⁻¹, ν (C=N) 1648 cm⁻¹, ν (C=N) (pyridine) 1572 cm⁻¹, ν (C=O) and 1651 cm⁻¹. ¹H NMR (500 MHz, DMSO) δ 8.57 (d, J = 75.9 Hz, 1H), 8.41 (s, 1H), 8.06 (d, J = 8.0 Hz, 1H), 7.88 (t, J = 6.5 Hz, 3H), 7.60 (t, J = 7.4 Hz, 1H), 7.52 (t, J = 7.6 Hz, 2H), 7.41 (dt, J = 31.4, 15.6 Hz, 1H), 2.06 (s, 1H). Anal. Calc. (%) For C₁₃H₁₁N₃O: C, 64.19; H, 5.39; N, 17.27. Found (%): C, 64.16; H, 5.33; N, 17.62.

Inhibition performance of corrosion inhibitors: Materials and electrolytes

Mild steel with surface area of 0.17 cm², 3.5% NaCl solution, CO₂ and N₂ to deoxygenate the solution [12]. Every experiment was carried out in unstirred, static solutions. Polishing Material, Potentiostat (Autolab, AUTO302N.FRA2 Netherlands), three electrode system glass cells with platinum electrode as counter electrode (CE), silver/silver chloride (Ag/AgCl) as reference electrode (RE) and mild steel as working electrode (WE). Tridentate hydrazone ligands (AL01 and AL02) were used as corrosion inhibitors.

Preparation of working electrode

The mild steel plate as working electrode was prepared by embedding the plate in epoxy resin, exposing a geometrical surface area of $0.17\,\mathrm{cm^2}$ in $1000\,\mathrm{mL}$ of 3.5% NaCl solution saturated with CO_2 gas at pH 4-4.3. The metal plate was polished using various grade of SiC paper (300, 500 and 4000) prior to each experiment and degreased with ethanol and acetone.

Electrochemical impedance spectroscopy measurement (EIS)

Impedance measurements were performed after 15 min immersion of the metal plate in static condition at steady state open circuit potential at 25 °C [20] with slight modification. It was conducted in conventional three-electrode cell using platinum as the counter electrode and Ag/AgCl as the reference electrode. The AC current frequency range extended from 10 kHz to 0.1 Hz with 10 mV peak-to-peak amplitude. Electrochemical impedance spectroscopy generated Nyquist and Bode plots where the calculation of corrosion inhibition efficiency (IE %) of the inhibitors were calculated based on the $R_{\rm p}$ values using Equation 1,

$$IE\% = \left(\frac{R_{p(inh)} - R_{p(blank)}}{R_{p(inh)}}\right) x \ 100 \tag{1}$$

where $R_{p(blank)}$ and $R_{p(inh)}$ are the resistance charge transfer for bare mild steel and after the presence of inhibitor [1].

Polarization measurement

The corrosion behavior was further investigated through potentiodynamic polarization, immediately after the impedance spectra were recorded on the same metal plate without any additional surface treatment. The potentials were scanned at a scan rate of 0.5 mVs⁻¹ from the corrosion potential (E_{corr}) in the cathodic direction and subsequently in the anodic direction. Potentiodynamic polarization gave the Tafel plot which was then extrapolated and corrosion inhibition efficiency (IE %) of the inhibitors was calculated based on the corrosion current density (i_{corr}) values using Equation 2,

$$IE\% = \left(\frac{i_{corr(0)} - i_{corr(i)}}{i_{corr(0)}}\right) x \ 100 \tag{2}$$

where $i_{corr(0)}$ and $i_{corr(i)}$ are the corrosion current densities for bare mild steel and after the presence of inhibitor [1].

Surface morphology analysis

The surface morphology and chemical composition were analyzed using scanning electron microscopy (SEM) coupled with energy dispersive X-ray spectroscopy (EDX) on the mild steel surfaces of samples that were immersed for 24 hours in 3.5% NaCl solution saturated with CO_2 , with and without the presence of inhibitor at optimal concentration (500 ppm) [21].

Results and Discussion

Physical properties and elemental analysis

Table 1 displays physical characteristics of both ligands, and the experimental percentages of the elements C, H, and N of the compounds are closely corresponded to the theoretical values which proved their stoichiometry.

Table 1. Physical data for tridentate hydrazone ligands

| Compound | Molecular Formula | Molecular Weight (g/mol) | Physical | Melting Point (°C) | Elemental Analysis Found (Calculated) (%) | | |
|----------|----------------------|--------------------------------|------------|--------------------------|--|------------------|---------|
| | | | Properties | | C | Н | N |
| AL01 | $C_{13}H_{11}N_3O_2$ | 241.25 | White | 225.8- | 65.21 | 4.66 | 17.75 |
| | | | | 227.3 | (64.72) | (4.60) | (17.42) |
| AL02 | $C_{13}H_{11}N_3O$ | 225.25 | Brown | 111.0- | 0- 64.16 5.33 | | 17.62 |
| | | | DIOWII | 113.6 | (64.19) | (64.19) (5.39) (| (17.27) |

Infrared spectroscopy

The infrared spectra for AL01 shown in Figure 1, exhibit strong peak for v(N-H), v(C=N), v(C=N) (pyridine), v(C=O) at 3242 cm⁻¹, 1608 cm⁻¹, 1542 cm⁻¹ and 1630 cm⁻¹, respectively. For AL02 spectra, the peaks for v(N-H), v(C=N), v(C=N) (pyridine), v(C=O) are at 3402 cm⁻¹, 1648 cm⁻¹, 1572 cm⁻¹, and 1651 cm⁻¹, respectively [22]. The stretching band for v(C=N) of pyridine was at the lower frequency region compared to aliphatic v(C=N) because of the N atom in the ring

acts as an activating and electron-donating group which causes the absorption band to move to a lower frequency region by pushing the electron clouds towards the ring and increasing the electron density [21]. There was a broad absorption band of O-H for AL01 that appeared in the region of 3000 cm⁻¹ [22]. Other prominent peaks for both ligands observed in Figure 1 are the C=C stretch (1466-1472 cm⁻¹), and the C-H sp² stretch (2925-2974 cm⁻¹), which indicate the existence of benzene rings in the structure [23].

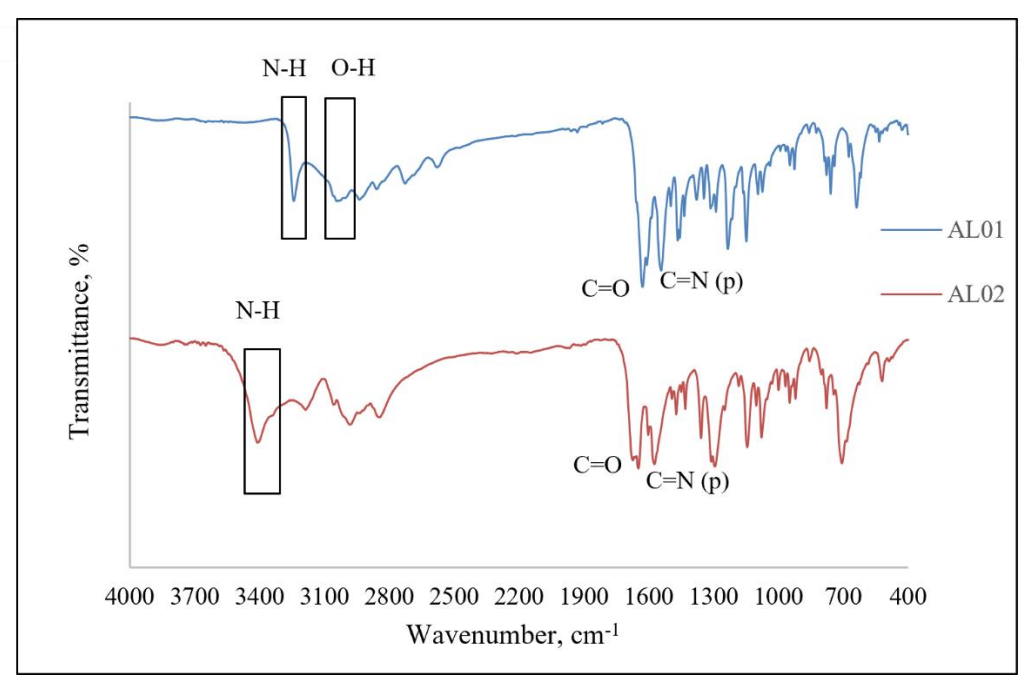


Figure 1. FTIR spectra of AL01 and AL02

Nuclear magnetic resonance spectroscopy

The ¹H NMR spectra for the ligand AL01 and AL02 were recorded in CDCl₃ and DMSO-d₆ respectively. Both ligands show a singlet peak at downfield region at 8.82 and 8.41 ppm, respectively, due to NH protons [24, 25] as shown in Figure 2(a) and Figure 2(b). For AL01 spectrum (Figure 2a), a singlet peak of phenolic proton appeared at 12.28 ppm strongly confirms the ligand structure [25]. The aromatic protons for benzene ring were observed in the range of 6.95-8.00 ppm for AL01 and in the range of 7.42-8.56 ppm for AL02 [26].

Ultraviolet-visible spectroscopy

The UV-Vis spectra of ligands AL01 and AL02 were measured at 5 x 10^{-5} M in acetonitrile between 190 to 450 nm. Two peaks in the absorption spectra of AL01 and AL02 in the range of 198-201 nm was due to the π - π *(C=C) transitions of aromatic rings [22]. However, for AL01 spectrum, there was a peak in the range of 205-210 nm which was assigned for n- π * transition as OH substituent at the *ortho* position was added to the benzene ring [27]. There was a weak band observed at 319 nm assigned for n- π * transition of C=N for AL01

while the peak for this transition was not found for AL02. There were also peaks of π - π * (C=N) transitions for AL01 at 302 nm and for AL02 at 299 nm. As shown in Figure 3, AL01 absorption is more bathochromic than AL02 because of the conjugated systems' effect from the OH functional group on the benzene ring. Hence, the absorption peaks appear at longer wavelengths compared to that of the benzene peak [27].

Liquid chromatography-mass spectrometry

The ligands AL01 and AL02 were characterized by LC-MS in the positive ion mode. When compared to the hypothesized structure, the mass spectrum of the ligand AL01 (Figure 4) exhibits a strong molecular ion peak at m/z = 242.09, which corresponds to the [C₁₃H₁₁N₃O₂]+H⁺ (calculated RMM of AL01 = 241.25). Based on AL02 spectrum, an additional support for the structure was provided by the intense molecular ion peak at m/z = 226.10 corresponding to [C₁₃H₁₁N₃O]+H⁺ which is in agreement with the molecular weight of the compound (225.25 g/mol) [28].

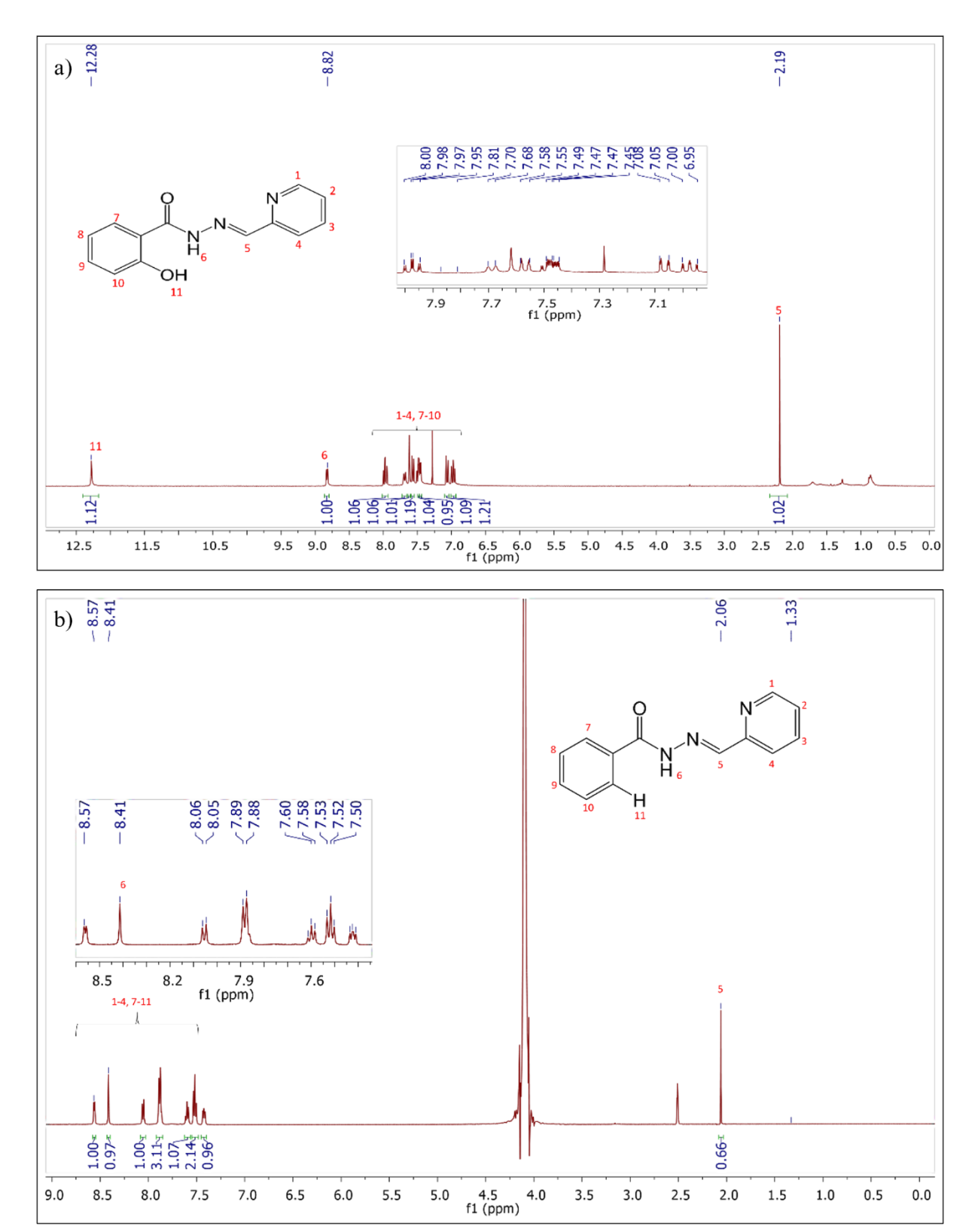


Figure 2. NMR spectra of a) AL01 and b) AL02

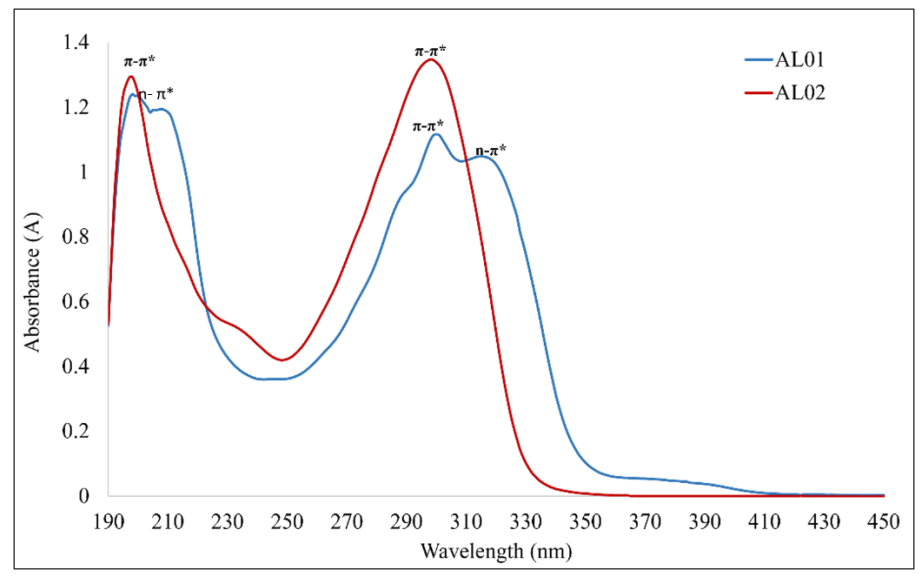
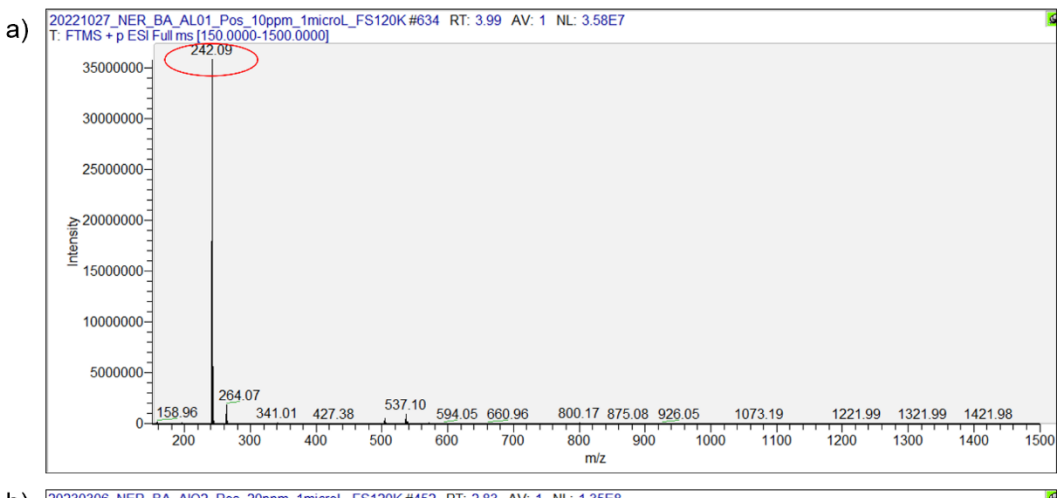


Figure 3. UV-Vis spectra of AL01 and AL02



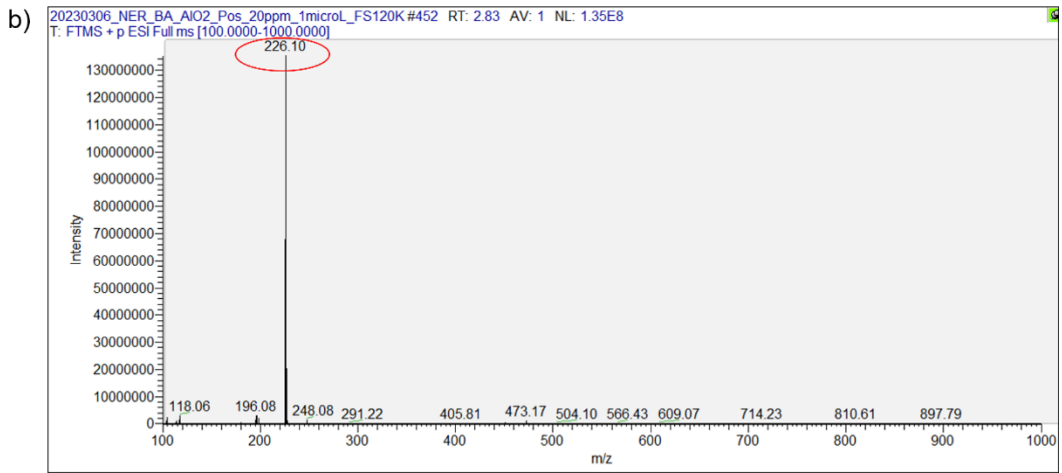


Figure 4. LC-MS spectra of a) AL01 and b) AL02

Inhibition performance of corrosion inhibitors: Potentiodynamic polarization (PDP)

Tafel extrapolation is a polarization technique to estimate corrosion rates that offers a faster alternative to traditional weight-loss method. The Tafel equation can be used to represent mixed potential theory using simple electrochemical kinetics, which can then be used to predict corrosion rate and potential based on the kinetics and thermodynamics of all reactions taking place on an electrode surface [29].

The potentiodynamic polarization parameters were computed using the Tafel extrapolation method. The corrosion rate values may be calculated using Equation 3, which is based on Faraday's equation [29]. Further on, the E_{corr} values were deducted from the intersection of the cathodic and anodic polarization curves [9].

$$CR (mpy) = \frac{0.00327 \times i_{corr} \times EW}{\rho}$$
 (3)

where i_{corr} is the corrosion current density in μA cm⁻², ρ is the density of the metal in g cm⁻³, EW is the equivalent weight. Table 2 shows the potentiodynamic polarization parameters for the 3.5% NaCl solution, and the solutions with the presence of inhibitors.

Table 2. Potentiodynamic polarization parameters for blank, with presence of inhibitors AL01 and AL02

| Compound | Concentration (ppm) | E _{corr} (V) | i _{corr} (μA/cm ²) | βa (V) | βc (V) | Corrosion Rate (mm/year) | Inhibition Efficiency (%) |
|----------|---------------------|-----------------------|--|--------|---------|--------------------------------|---------------------------------|
| Blank | 3.5% NaCl | -0.6509 | 83.659 | 0.0502 | -6.3902 | 0.9834 | - |
| | 100 | -0.6134 | 58.795 | 0.0356 | 0.1279 | 0.6912 | 30.00 |
| | 200 | -0.5889 | 47.904 | 0.0300 | 0.1602 | 0.5631 | 42.74 |
| AL01 | 300 | -0.6177 | 35.347 | 0.0618 | 0.2486 | 0.4155 | 57.75 |
| | 400 | -0.6721 | 32.938 | 0.0409 | 0.3625 | 0.3872 | 60.63 |
| | 500 | -0.6110 | 13.132 | 0.0463 | 0.2081 | 0.1544 | 84.30 |
| | 100 | -0.6583 | 43.790 | 0.0607 | 0.4808 | 0.5148 | 47.66 |
| | 200 | -0.6989 | 38.570 | 0.0632 | 0.2813 | 0.4534 | 53.90 |
| AL02 | 300 | -0.6733 | 34.502 | 0.0423 | 0.3106 | 0.4056 | 58.76 |
| | 400 | -0.6729 | 34.025 | 0.0665 | 0.2524 | 0.4000 | 59.33 |
| | 500 | -0.6426 | 21.002 | 0.0415 | 0.3638 | 0.2469 | 74.90 |

All data tabulated in Table 2 were originally obtained from Tafel plot as shown in Figure 5 below. It revealed that uncoated mild steel plate had the highest corrosion current density (i_{corr}), $83.659~\mu A/cm^2$ and was therefore more prone to corrosion (active dissolution) [9]. Table 2 shows that there was a significant reduction in the corrosion current densities (i_{corr}) with increasing inhibitor concentration. In the presence of AL01 inhibitor, the value of i_{corr} decreased from 58.795 $\mu A/cm^2$ to 13.132 $\mu A/cm^2$, while in the presence of AL02, the value decreased from 43.790 $\mu A/cm^2$ to 21.002 $\mu A/cm^2$.

This was an obvious indication of how increasing

inhibitor concentration resulted in an increasing number of hydrazone molecules to be adsorbed on the mild steel surface, inhibiting all forms of corrosion that were present at the metal-electrolyte interface [30]. The data proved that both inhibitors had an inhibitory impact on the aggressive mild steel solution, which effectively blocked the active site while the inhibitor was adsorbing to the mild steel surface [31]. Additionally, PDP data (Table 2) show that AL01 exhibits the highest level of inhibition, with an inhibition efficiency of 84.30%, followed by AL02 (74.90%).

This result was supported by the presence of OH functional group on the benzene ring in AL01 that could

Hisyam et al.: INHIBITION EFFECTS OF TRIDENTATE HYDRAZONE LIGANDS AS CORROSION INHIBITORS ON MILD STEEL IN SATURATED CO, ENVIRONMENT

enhance the adsorption process on the mild steel by increasing the molecule's electron charge density and molecule's binding affinity with the steel surface [12].

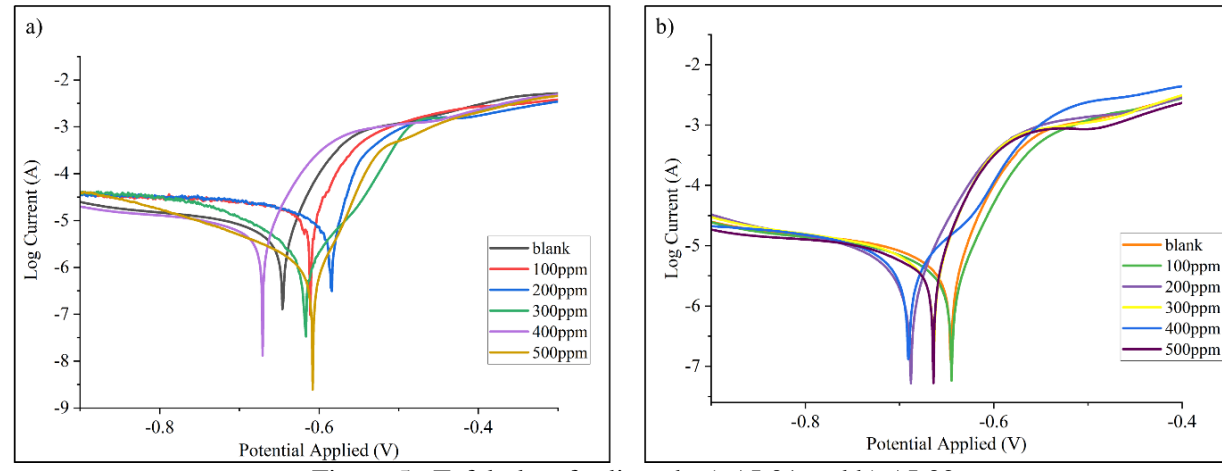


Figure 5. Tafel plots for ligands a) AL01 and b) AL02

The findings from Tafel plots (Figure 5) provided a helpful comparison of changes in potential corrosion values and the degree of corrosion current density reduction. This indicates that the corrosion reactions are inhibited [12]. When carbon dioxide gas dissolved in aqueous media, carbonic acid (H₂CO₃) was produced. Then, the bicarbonate ion (which could further dissociate to produce the carbonate ion) formed when the carbonic acid (H₂CO₃) partially dissociated. It has been widely recognized that, at the same pH, solutions containing H₂CO₃ would corrode mild steel more severely than solutions containing strong acids i.e., hydrochloric (HCl) or sulfuric (H₂SO₄) acids as they act as an additional source of hydrogen ions thus, lead to higher corrosion rates [11, 32].

Electrochemical impedance spectroscopy (EIS)

In addition, electrochemical impedance measurements were carried out to investigate the mechanisms of interaction between the electrode surface and the chemicals being studied, such as charge transfer,

diffusion, and adsorption. Inhibitor adsorption on the metal substrate was corroborated by EIS studies, which also showed a rise in polarization resistance as the concentration of inhibitors increased [15]. Figure 6 shows Nyquist plots for mild steel at various concentrations of AL01 and AL02, in 3.5% NaCl solution saturated with CO₂.

-0.4

Apparently, incomplete single depressed capacitive loops with nearly the same forms, both with and without inhibitors make up Nyquist plots, which show that the corrosion mechanism remains the same [17]. The nonhomogeneity or roughness of the metal surface and the resistance to mass movement were the causes of the Nyquist plot's deviation from perfect semicircles, which was known as frequency dispersion. The semi-circle curve's diameter increased as the inhibitor concentration increased, demonstrating the inhibitor's ability to bind to mild steel forming a protective film over the metal surface [12, 31].

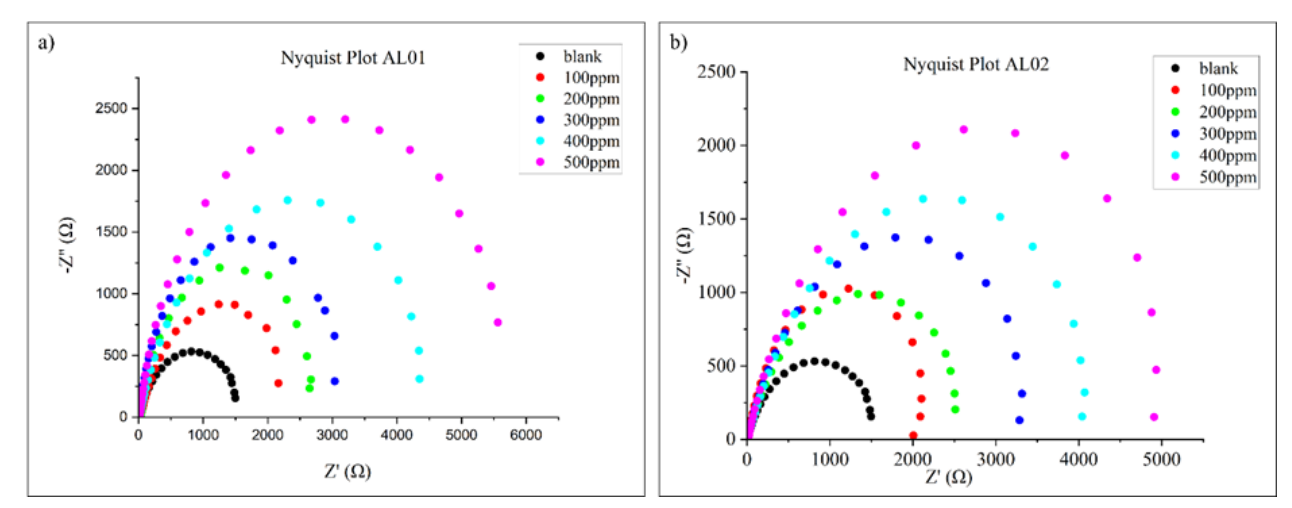


Figure 6. Nyquist plots for ligands a) AL01 and b) AL02

A basic Randle's circuit proposed in Figure 7 can be employed to represent the semi-circle Nyquist plots that were generated through the experiment. This circuit

demonstrated that the charge transfer resistance (Rp) is parallel to the constant phase element (CPE) in series with the solution resistance (Rs) [31].

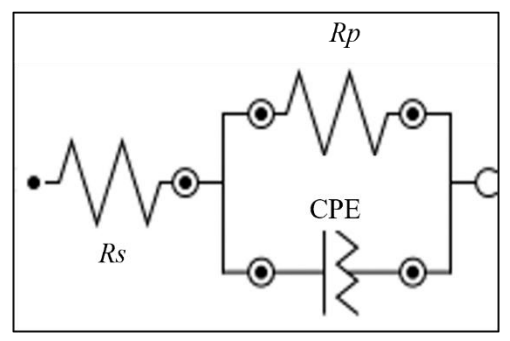


Figure 7. Simple Randle's circuit

Nyquist plots (Figure 6), indicate the samples' capacitive behavior, which consists of a single capacitive loop. The diameter of the Nyquist diagram represents the treated mild steel substrate's corrosion resistance (Rp, as indicated in EIS), which is correlated with the rate of corrosion. A greater semicircle diameter is indicative of a higher corrosion resistance, or a lower rate of corrosion. The resultant capacitive loop demonstrates that the charge transfer mechanism and the formation of a corrosion-inhibitory layer on the mild steel surface control the corrosion of mild steel in a 3.5% NaCl solution [9].

The impedance parameters obtained from Nyquist plots

are presented in Table 3. The observed *Rp* values exhibited a significant increase in the presence of inhibitors, particularly at higher concentrations, in comparison to the *Rp* value obtained without the presence of an inhibitor. Consequently, the corrosion inhibition efficiency exhibited an increase. This behavior confirmed the formation of the protective film on mild steel. The observed trend in the diameter of the semi-circle curve indicates a positive correlation with the concentration of the inhibitor, hence, suggesting the occurrence of adsorption of the inhibitor on mild steel. This prevents the mild steel from corroding because the adsorbed layer formed hinders charge and mass transfers at the metal-inhibitor solution interface [31].

| Compound | Concentration | Rs | R _{ct} | Inhibition Efficiency | | |
|----------|---------------|------------|-----------------|-----------------------|--|--|
| Compound | (ppm) | (Ω) | (Ω) | (%) | | |
| Blank | - | 10.8 | 1596 | - | | |
| | 100 | 29.8 | 2461 | 35.15 | | |
| | 200 | 35.84 | 2802 | 43.04 | | |
| AL01 | 300 | 16.9 | 3760 | 57.55 | | |
| | 400 | 13.1 | 4749 | 66.39 | | |
| | 500 | 19.4 | 5883 | 72.87 | | |
| | 100 | 12.7 | 2185 | 26.96 | | |
| | 200 | 11.0 | 2781 | 42.61 | | |
| AL02 | 300 | 11.9 | 3700 | 56.86 | | |
| | 400 | 10.5 | 4545 | 64.88 | | |
| | 500 | 14.7 | 5529 | 71.13 | | |

Table 2. Impedance parameter values for the corrosion of mild steel

The Nyquist plots and impedance data presented in Table 3 indicate that the corrosion resistance of both inhibitors was found to be improved by increasing the concentration to 500 ppm. The mild steel immersed in 3.5% NaCl solution with 500 ppm inhibitors produced the biggest semi-circle diameter, as shown in Figure 6. Furthermore, comparing AL01 and AL02, the diameter of the Nyquist plot was bigger for AL01 at 500 ppm suggesting a better corrosion resistance i.e., a more robust inhibitive layer [9].

SEM-EDX Analysis

Scanning electron microscopy (SEM) was employed to examine the morphology of the metal surface and the development of the protective film on the surface of mild steel. Following the inhibitors' binding, the steel surface was seen to be smoother [33]. Figure 8 shows the SEM micrographs for mild steel after 24 hours immersion in 3.5% NaCl solution with and without the presence of corrosion inhibitors.

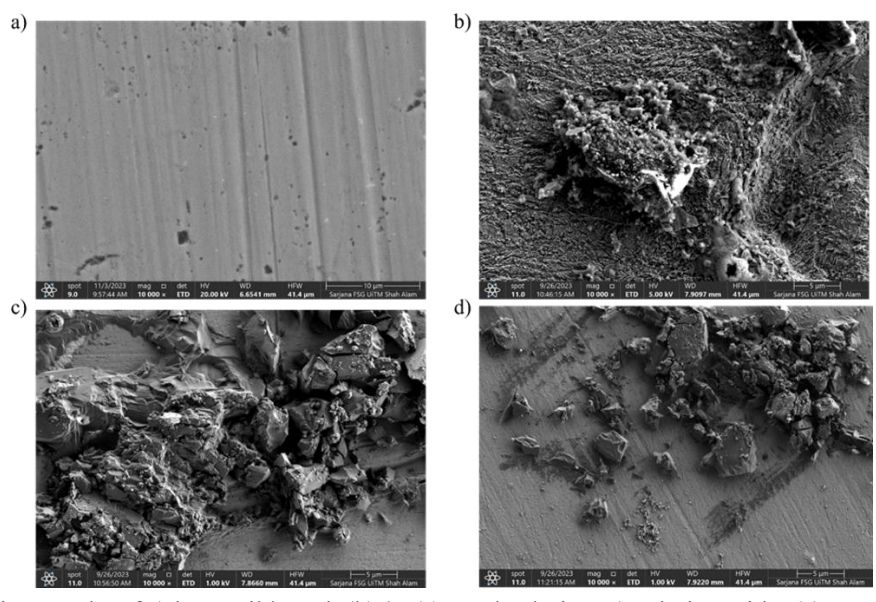


Figure 8. SEM micrographs of a) bare mild steel, (b) 3.5% NaCl solution, c) solution with 500 ppm of AL01 and d) solution with 500 ppm of AL02

Due to the manual abrasion process used during the polishing phase of the panels, scratch marks were apparent on the mild steel's exposed surface [9]. From observation, untreated mild steel plate in 3.5% NaCl solution (blank) (b) had a much rougher surface compared to surfaces with the presence of AL01 and AL02, which were substantially smoother. SEM examination confirmed that the presence of hydrazone ligands in the solution offered efficient corrosion retardation with the least amount of surface damage [9]. This is due to the formation of an adsorption layer that minimizes the effects of corrosion although the steel's surface treatment still left some residual scratches and polishing lines as in Figure 8(a) [34].

Energy dispersive X-ray spectroscopy (EDX) was used to evaluate the protective mechanism of inhibitors to find reductions in peaks related to iron, carbon, and chloride which are markers for metal corrosion [33]. According to the EDX study (Table 4), Fe, C and small traces of Si were detected as elements in bare mild steel. Noticeably, Fe content was decreased when treated with

AL01 and AL02 from 97.25% to 82.19 wt.% and 95.35 wt.% respectively. This indicates the adsorption of inhibitors on the surface of the mild steel thus, reducing the Fe content [9]. For untreated mild steel there was a presence of Cl, signifying a corrosion attack from NaCl solution in aggressive environment [35]. However, when comparing the weight percentage (wt.%) (Table 4) of Cl element in the presence of inhibitors with that of the blank, there was no Cl detected when the inhibitors were present. This observation demonstrates the adsorption of inhibitors on the mild steel surface where elements such as C, N and O correspond to the inhibitor's composition, which were found on the mild steel immersed in the presence of AL01 and AL02 inhibitors. These are essential for stabilizing the molecule at the surface, which enhance the ability of the steel to resist corrosion [33, 35]. Hence, compared to AL02, which agrees with the data in Table 4, AL01 had a higher capacity to build a protective film corrosion because of its strong electron-donating ability due to the presence of OH functional group [19].

Table 3. Weight percentage of elements in mild steel specimen obtained from EDX spectra

| Mild Steel Specimen | Fe (wt.%) | C (wt.%) | Si (wt.%) | Cl (wt.%) | Na (wt.%) | O (wt.%) | N (wt.%) |
|----------------------|--------------|-------------|--------------|--------------|--------------|-------------|-------------|
| Bare mild steel | 97.25 | 2.10 | 0.65 | - | - | - | - |
| Untreated mild steel | 75.51 | 1.89 | _ | 6.28 | 15.37 | 0.95 | - |
| Treated with AL01 | 82.19 | 13.60 | _ | _ | _ | 2.47 | 1.74 |
| Treated with AL02 | 95.35 | 3.23 | - | - | - | 1.07 | 0.35 |

Conclusion

New corrosion inhibitors of tridentate hydrazone ligands, AL01 and AL02 were successfully synthesized via condensation process derived from two different substituents of hydrazides. The ligands were characterized using FTIR, NMR, elemental analysis, mass spectroscopy and UV-Vis. From polarization and EIS study, it can be concluded that AL01 has the highest inhibition efficiency, 84.30% at 500 ppm compared to 74.90% of AL02. SEM-EDX analysis has confirmed the formation of inhibitors' layer on mild steel as the surface of the mild steel with the presence of inhibitors is smoother compared to that of the untreated mild steel in 3.5% NaCl solution saturated with CO₂. Hence, compared to AL02, AL01 has a higher inhibitory

efficacy and the compound formed a stronger protective layer on the mild steel as the compound contains electron donating group (OH).

Acknowledgement

The authors express their gratitude to the Malaysian Ministry of Higher Education for providing the research funding under the grant FRGS/1/2021/STG04/UITM/02/21. Additionally, the authors would like to acknowledge the support and research facilities provided by Universiti Teknologi MARA Shah Alam and AuRIns, UiTM Puncak Alam.

References

1. Mashitah A., N., Athena Z., F. and Hazwan H., M.

Hisyam et al.: INHIBITION EFFECTS OF TRIDENTATE HYDRAZONE LIGANDS AS CORROSION INHIBITORS ON MILD STEEL IN SATURATED CO₂ ENVIRONMENT

- (2021). The study of electroless Ni-Cu-P plating on corrosion resistance of aluminium in 3.5% NaCl physicochemical characteristics of microcrystalline cellulose and cellulose nanowhiskers from lignocellulosic biomass. *International Journal Electroactive Materials*, 9: 12-26.
- 2. Sulzer Pumps. (2010). Materials and corrosion. *Centrifugal Pump Handbook*: pp. 227-250.
- 3. Jafar M. M. A. (2020). Global impact of corrosion: Occurrence, cost and mitigation. *Global Journal of Engineering Sciences*, 5(4): 1-4.
- 4. Tamalmani, K. and Husin, H. (2020). Review on corrosion inhibitors for oil and gas corrosion issues. *In Applied Sciences*, 10(10): 3389,
- Adam, M. S. S., Soliman, K. A. and Abd El-Lateef, H. M. (2020). Homo-dinuclear VO²⁺ and Ni²⁺ dihydrazone complexes: Synthesis, characterization, catalytic activity and CO₂corrosion inhibition under sustainable conditions. *Inorganica Chimica Acta*, 499(9): 119212.
- Askari, M., Aliofkhazraei, M. and Afroukhteh, S. (2019). A comprehensive review on internal corrosion and cracking of oil and gas pipelines. *Journal of Natural Gas Science and Engineering*, 71: 102971.
- Oyekunle, D. T., Agboola, O. and Ayeni, A. O. (2019). Corrosion inhibitors as building evidence for mild steel: A review. *Journal of Physics: Conference Series*, 1378(3).
- Usman, B. J., Umoren, S. A. and Gasem, Z. M. (2017). Inhibition of API 5L X60 steel corrosion in CO₂-saturated 3.5% NaCl solution by tannic acid and synergistic effect of KI additive. *Journal of Molecular Liquids*, 237: 146-156.
- Hamidon, T. S. and Hussin, M. H. (2020). Susceptibility of hybrid sol-gel (TEOS-APTES) doped with caffeine as potent corrosion protective coatings for mild steel in 3.5 wt.% NaCl. *Progress* in *Organic Coatings*, 140: 105478.
- Lin, B., Tang, J., Wang, Y., Wang, H. and Zuo, Y. (2020). Study on synergistic corrosion inhibition effect between calcium lignosulfonate (CLS) and inorganic inhibitors on Q235 carbon steel in alkaline environment with Cl-. *Molecules*, 25(18): 4200.
- 11. George, K. S. and Nes, S. (1944). Investigation of

- carbon dioxide corrosion of mild steel in the presence of acetic acid-part 1: basic mechanisms. *Corrosion Science Section Corrosion-February* 2007: 1-30.
- Singh, A., Ansari, K. R., Xu, X., Sun, Z., Kumar, A. and Lin, Y. (2017). An impending inhibitor useful for the oil and gas production industry: Weight loss, electrochemical, surface and quantum chemical calculation. *Scientific Reports*, 7(1): 14904.
- Das Chagas Almeida, T., Bandeira, M. C. E., Moreira, R. M. and Mattos, O. R. (2017). New insights on the role of CO₂ in the mechanism of carbon steel corrosion. *Corrosion Science*, 120: 239-250.
- Chaouiki, A., Chafiq, M., Lgaz, H., Al-Hadeethi, M. R., Ali, I. H., Masroor, S. and Chung, I. M. (2020). Green corrosion inhibition of mild steel by hydrazone derivatives in 1.0 M HCl. *Coatings*, 10(7): 1-17.
- 15. Saady, A., Rais, Z., Benhiba, F., Salim, R., Ismaily Alaoui, K., Arrousse, N., Elhajjaji, F., Taleb, M., Jarmoni, K., Kandri Rodi, Y., Warad, I. and Zarrouk, A. (2021). Chemical, electrochemical, quantum, and surface analysis evaluation on the inhibition performance of novel imidazo[4,5-b] pyridine derivatives against mild steel corrosion. *Corrosion Science*, 189(7): 109621.
- Subbiah, K., Lee, H.-S., Al-Hadeethi, M. R., Park, T. and Lgaz, H. (2023). Unraveling the anticorrosion mechanisms of a novel hydrazone derivative on steel in contaminated concrete pore solutions: An integrated study. *Journal of Advanced Research*, 8: 16.
- 17. Khamaysa, O. M. A., Selatnia, I., Zeghache, H., Lgaz, H., Sid, A., Chung, I. M., Benahmed, M., Gherraf, N., and Mosset, P. (2020). Enhanced corrosion inhibition of carbon steel in HCl solution by a newly synthesized hydrazone derivative: Mechanism exploration from electrochemical, XPS, and computational studies. *Journal of Molecular Liquids*, 315: 113805.
- Ansari, K. R., Chauhan, D. S., Singh, A., Saji, V. S. and Quraishi, M. A. (2020). Corrosion inhibitors for acidizing process in oil and gas sectors. *Corrosion Inhibitors in the Oil and Gas Industry*, 2020: 153-

176.

- Khamaysa, O. M. A., Selatnia, I., Lgaz, H., Sid, A., Lee, H. S., Zeghache, H., Benahmed, M., Ali, I. H. and Mosset, P. (2021). Hydrazone-based green corrosion inhibitors for API grade carbon steel in HCl: Insights from electrochemical, XPS, and computational studies. *Colloids and Surfaces A: Physicochemical and Engineering Aspects*, 626: 127047.
- Boukazoula, S., Haffar, D., Bourzami, R., Toukal, L. and Dorcet, V. (2022). Synthesis, characterizations, crystal structure, inhibition effects and theoretical study of novel Schiff base on the corrosion of carbon steel in 1 M HCl. *Journal of Molecular Structure*, 1261: 132852.
- Kamal, N. K. M., Fadzil, A. H., Kassim, K., Rashid,
 S. H. and Mastuli, M. S. (2014). Synthesis, characterization and corrosion inhibition studies of o, m, p-decanoyl thiourea derivatives on mild steel in 0.1 M H₂SO₄ solutions. *Malaysian Journal of Analytical Sciences*, 18(1): 21-27.
- Latifah R., H., Bahron, H., Ramasamy, K. and Tajuddin, A. M. (2019). Synthesis and characterization of benzohydroxamic acid and methylbenzohydroxamic acid metal complexes and their cytotoxicty study. *Malaysian Journal of Analytical Sciences*, 23(2), 263-273.
- 23. Shahrul Nizam, A., Bahron, H. and Tajuddin, A. M. (2019). Effect of temperature on the catalytic activity of new symmetrical tetradentate palladium(II) schiff base complexes in copper-free sonogashira reaction. *Malaysian Journal of Analytical Sciences*, 23(2): 247-254.
- Gao, H., Li, J. Q., Kang, P. W., Chigan, J. Z., Wang, H., Liu, L., Xu, Y. S., Zhai, L. and Yang, K. W. (2021). N-acylhydrazones confer inhibitory efficacy against New Delhi metallo-β-lactamase-1. *Bioorganic Chemistry*, 114: 105138.
- 25. Kant, R., Yang, M. H., Tseng, C. H., Yen, C. H., Li, W. Y., Tyan, Y. C., Chen, M., Tzeng, C. C., Chen, W. C., You, K., Wang, W. C., Chen, Y. L. and Chen, Y. M. A. (2021). Discovery of an orally efficacious MYC inhibitor for liver cancer using a GNMT-based high-throughput screening system and structure-activity relationship analysis. *Journal of Medicinal Chemistry*, 64(13): 8992-9009.

- 26. Singh, Y., Patel, R. N., Patel, S. K., Patel, A. K., Patel, N., Singh, R., Butcher, R. J., Jasinski, J. P. and Gutierrez, A. (2019). Experimental and quantum computational study of two new bridged copper(II) coordination complexes as possible models for antioxidant superoxide dismutase: Molecular structures, X-band electron paramagnetic spectra and cryogenic magnetic properties. *Polyhedron*, 171: 155-171.
- 27. Bononi, F. C., Chen, Z., Rocca, D., Andreussi, O., Hullar, T., Anastasio, C. and Donadio, D. (2020). Bathochromic shift in the UV-visible absorption spectra of phenols at ice surfaces: Insights from first-principles calculations. *Journal of Physical Chemistry A*, 124(44): 9288-9298.
- Khaidir, S. S., Bahron, H., Tajuddin, A. M. and Ramasamy, K. (2022). Microwave-assisted synthesis, characterization and anticancer activity of tetranuclear Schiff base complexes. *Journal of Sustainability Science and Management*, 17(4): 32-48.
- 29. Kakaei, K., Esrafili, M. D. and Ehsani, A. (2019). Graphene and anticorrosive properties. *In Interface Science and Technology*, (Vol. 27, pp. 303-337). Elsevier.
- Lgaz, H., Chung, I. M., Albayati, M. R., Chaouiki, A., Salghi, R. and Mohamed, S. K. (2020). Improved corrosion resistance of mild steel in acidic solution by hydrazone derivatives: An experimental and computational study. *Arabian Journal of Chemistry*, 13(1): 2934-2954.
- 31. Hazani, N. N., Mohd, Y., Ghazali, S. A. I. S. M. and Dzulkifli, N. N. (2019). Electrochemical studies of thiosemicarbazone derivative and its tin(IV) complex as corrosion inhibitor for mild steel in 1 M hydrochloric acid. *Chemistry Journal of Moldova*, 14(1): 98-106.
- 32. Rustandi, A., Adyutatama, M., Fadly, E. and Subekti, N. (2012). Corrosion rate of carbon steel for flowline and pipeline as transmission pipe in natural gas production with CO₂ content. *Makara Journal of Technology*, 16(1): 57-62.
- Chafiq, M., Chaouiki, A., Al-Hadeethi, M. R., Ali, I. H., Mohamed, S. K., Toumiat, K. and Salghi, R. (2020). Naproxen-based hydrazones as effective corrosion inhibitors for mild steel in 1.0 M HCl.

Hisyam et al.: INHIBITION EFFECTS OF TRIDENTATE HYDRAZONE LIGANDS AS CORROSION INHIBITORS ON MILD STEEL IN SATURATED CO₂ ENVIRONMENT

- Coatings, 10(7): 700.
- 34. Lgaz, H., Chaouiki, A., Albayati, M. R., Salghi, R., El Aoufir, Y., Ali, I. H., Khan, M. I., Mohamed, S. K. and Chung, I. M. (2019). Synthesis and evaluation of some new hydrazones as corrosion inhibitors for mild steel in acidic media. *Research on Chemical Intermediates*, 45(4): 2269-2286.
- 35. El-Haddad, M. A. M., Bahgat Radwan, A., Sliem, M. H., Hassan, W. M. I. and Abdullah, A. M. (2019). Highly efficient eco-friendly corrosion inhibitor for mild steel in 5 M HCl at elevated temperatures: experimental & molecular dynamics study. *Scientific Reports*, 9(1): 1-15.